

Anti-plane shear waves in an elastic strip rigidly attached to an elastic half-space

Gennadi Mikhasev^a, Barış Erbaş^b, Victor A. Eremeyev^{c,d,*}

^a*Department of Bio- and Nanomechanics, Faculty of Mechanics and Mathematics, Belarusian State University, Nezavisimosty Ave., 4, 220030 Minsk, Belarus*

^b*Department of Mathematics, Eskisehir Technical University Yunus Emre Campus, 26470, Eskisehir, Turkey*

^c*Department of Civil and Environmental Engineering and Architecture (DICAAR), University of Cagliari, Via Marengo, 2, 09123 Cagliari, Italy*

^d*Faculty of Civil and Environmental Engineering, Gdańsk University of Technology, ul. Gabriela Narutowicza 11/12 80-233 Gdańsk, Poland*

Abstract

We consider the anti-plane shear waves in a domain consisting of an infinite layer with thin coating lying on an elastic half-space. The elastic properties of both part are assumed to be different. On the free upper surface, the compatibility condition within the Gurtin–Murdoch surface elasticity is assumed, whereas at the plane interface we consider perfect contact conditions. For this problem there exists two possible regimes related to waves exponentially decaying in the half-space. The first one, called TE-TE regime, is related to waves described by exponential in transverse direction functions; the second, TH-TE regime, corresponds to waves which have the harmonic behaviour in the transverse direction in the upper layer. Detailed analysis of the derived dispersion equations for both regimes is provided. In particular, the effects of surface stresses, the layer thickness as well as of the ratio of shear moduli of the upper layer and half-space on the dispersion curves is analyzed.

Keywords: surface elasticity, anti-plane waves, dispersion relations, harmonic and exponential regimes, elastic layer on a half-space

*Corresponding author.

Email addresses: mikhasev@bsu.by (Gennadi Mikhasev), berbas@eskisehir.edu.tr (Barış Erbaş), eremeyev.victor@gmail.com (Victor A. Eremeyev)

Introduction

Following Eremeyev et al. (2016); Mikhasev et al. (2022) in this paper we discuss anti-plane surface waves in a multilayered medium which consists of thin coating modelled within the Gurtin–Murdoch surface elasticity, an elastic layer of finite thickness perfectly attached to an elastic half-space (Fig. 1). From the physical point of view, this medium describes a three-layered medium with thickness of layers of thickness of different order of magnitude. For example, it may describe a thin film with modified surface properties attached to a substrate. The considered layered medium generalizes recent results by Mikhasev et al. (2022) towards more realistic behaviour of substrate, which is now deformable and can transmit waves.

The paper is organized as follows. In Section 1 we formulate the statement of the problem under consideration in the case of anti-plane motions. For the layer two types of solutions are possible, that are expressed through exponential and harmonic (trigonometric) functions, respectively. We call these solutions transverse exponential (TE) and transverse harmonic (TH), respectively. As in Eremeyev et al. (2016), for the half-space there is only exponentially decaying solutions. Detailed analysis of TE solutions is given in Section 2, whereas harmonic waves are analyzed in Section 3. Finally, in Section 4 we provide detailed analysis of dispersion curves.

1. Setting the problem within linear Gurtin–Murdoch surface elasticity

Let us consider a three-dimensional elastic isotropic plate-like body of thickness h rigidly attached to an elastic isotropic half-space. The origin of the used Cartesian coordinate system is chosen at the interface as shown in Fig. 1.

To study anti-plane waves we assume the vector of displacement \mathbf{u} in the form, see, *e.g.*, Achenbach (1973),

$$\mathbf{u} = \mathbf{u}(x_1, x_2, x_3, t) = u(x_1, x_2, t)\mathbf{i}_3, \quad (1)$$

where t is time and \mathbf{i}_i are the base vectors, $i = 1, 2, 3$, see Fig. 1. In what follows we restrict ourselves to isotropic homogeneous materials. So using Hooke’s law for the anti-plane shear in both the plate and half-space, we

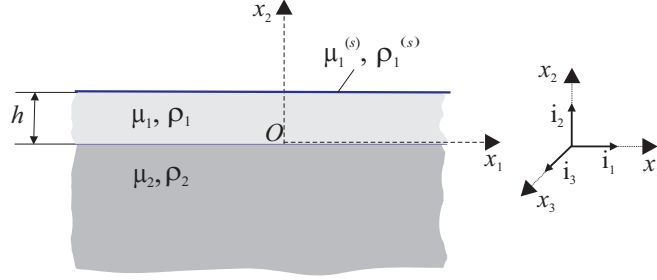


Figure 1: Infinite elastic plate-like domain lying on elastic half-space and used Cartesian coordinate system.

obtain

$$\begin{aligned}\boldsymbol{\sigma} &= 2\mu_j \mathbf{e} = \sigma_{13}(\mathbf{i}_1 \otimes \mathbf{i}_3 + \mathbf{i}_3 \otimes \mathbf{i}_1) + \sigma_{23}(\mathbf{i}_2 \otimes \mathbf{i}_3 + \mathbf{i}_3 \otimes \mathbf{i}_2), \\ \sigma_{13} &= 2\mu_j \varepsilon_{13}, \quad \sigma_{23} = 2\mu_j \varepsilon_{23}, \quad j = 1, 2,\end{aligned}\quad (2)$$

where $\boldsymbol{\sigma}$ and \mathbf{e} are the stress and strain tensors, respectively, and μ_j is a shear modulus, which will be assumed to be different for the upper layer and half-space (μ_1 and μ_2 , respectively). Hereinafter, the subscripts $j = 1$ and $j = 2$ correspond to the upper layer and half-space, respectively. Taking into account (1), the strain tensor reads

$$\begin{aligned}\mathbf{e} &= \varepsilon_{13}(\mathbf{i}_1 \otimes \mathbf{i}_3 + \mathbf{i}_3 \otimes \mathbf{i}_1) + \varepsilon_{23}(\mathbf{i}_2 \otimes \mathbf{i}_3 + \mathbf{i}_3 \otimes \mathbf{i}_2), \\ \varepsilon_{13} &= \frac{1}{2} \frac{\partial u}{\partial x_1}, \quad \varepsilon_{23} = \frac{1}{2} \frac{\partial u}{\partial x_2}.\end{aligned}\quad (3)$$

Here \otimes stands for the dyadic product.

As a result, equations of motion for the two parts of the continuum take the form of wave equations Achenbach (1973)

$$\mu_j \left(\frac{\partial^2 u_j}{\partial x_1^2} + \frac{\partial^2 u_j}{\partial x_2^2} \right) = \rho_j \frac{\partial^2 u_j}{\partial t^2}, \quad j = 1, 2, \quad (4)$$

where ρ_j is the mass density in the bulk.

In what follows, we consider the following boundary conditions. On the free surface $x_2 = h$, the compatibility condition within the Gurtin-Murdoch model of the surface elasticity is assumed Gurtin & Murdoch (1975):

$$\mu_1 \frac{\partial u_1}{\partial x_2} = \mu_1^{(s)} \frac{\partial^2 u_1}{\partial x_1^2} - \rho_1^{(s)} \frac{\partial^2 u_1}{\partial t^2} \quad \text{at } x_2 = h, \quad (5)$$

where $\mu_1^{(s)}$ and $\rho_1^{(s)}$ are surface shear modulus and density, respectively. At the interface $x_2 = 0$, we consider the perfect contact which is expressed by two equations, namely,

$$u_1 = u_2 \quad \text{at} \quad x_2 = 0, \quad (6)$$

$$\mu_1 \frac{\partial u_1}{\partial x_2} = \mu_2 \frac{\partial u_2}{\partial x_2} \quad \text{at} \quad x_2 = 0. \quad (7)$$

Also, for the half-space, we set the wave attenuation condition at infinity,

$$u_2 \longrightarrow 0 \quad \text{as} \quad x_2 \longrightarrow -\infty. \quad (8)$$

In the recently published contribution Mikhasev et al. (2022), an analysis of the wave equation similar to (4) for a plate with at least one free surface revealed the existence of two different regimes of anti-plane shear waves: (a) the TE regime for which waves decay exponentially from the upper and lower surfaces of the plate and (b) the TH regime with the harmonic behaviour of waves in the transverse direction. A similar analysis of Eqs. (4) for our problem shows that there exist both the TE and TH regimes in the plate and only the TE regime in the half-space. Here, we refer to these regimes as TE-TE and TH-TE, respectively.

2. TE-TE regime of anti-plane waves

Consider the TE-TE regime for which the amplitudes of anti-plane waves decay exponentially from the upper surface of the plate and from the interface in both directions. For this regime, a solution of Eqs. (4) can be sought in the form

$$u_1 = e^{i(kx_1 - \omega t)} (a_1 e^{\alpha_1(x_2 - h_1)} + a_2 e^{-\alpha_1 x_2}), \quad u_2 = b e^{i(kx_1 - \omega t)} e^{\alpha_2 x_2}, \quad (9)$$

where $i = \sqrt{-1}$, k is a wave number, ω is the circular frequency, and a_1, a_2, b are constants that have to be determined from the boundary conditions.

Substituting (9) in Eqs. (4) for $j = 1, 2$, we find

$$\alpha_1 = |k| \sqrt{1 - c^2/c_{T1}^2}, \quad \alpha_2 = |k| \sqrt{1 - c^2/c_{T2}^2} \quad (10)$$

with

$$c = \frac{\omega}{k}, \quad c_{T1} = \sqrt{\frac{\mu_1}{\rho_1}} \quad \text{and} \quad c_{T2} = \sqrt{\frac{\mu_2}{\rho_2}}, \quad (11)$$

where c is the phase velocity, and c_{T1}, c_{T2} are the shear wave speeds in the upper layer and the half-space, respectively. Here, $c < c_{T1}$, $c < c_{T2}$.

Substituting (9) into the boundary conditions (5)–(7) and using (10), we arrive at the dispersion equation

$$\begin{aligned} & \left(\frac{1}{|k|l_d} \sqrt{1 - \frac{c^2}{c_{T1}^2}} + \frac{c_s}{c_{T1}^2} - \frac{c^2}{c_{T1}^2} \right) \left(\mu_2 \sqrt{1 - \frac{c^2}{c_{T2}^2}} + \mu_1 \sqrt{1 - \frac{c^2}{c_{T1}^2}} \right) \\ & + \left(\frac{1}{|k|l_d} \sqrt{1 - \frac{c^2}{c_{T1}^2}} - \frac{c_s}{c_{T1}^2} + \frac{c^2}{c_{T1}^2} \right) \left(\mu_2 \sqrt{1 - \frac{c^2}{c_{T2}^2}} \right. \\ & \left. - \mu_1 \sqrt{1 - \frac{c^2}{c_{T1}^2}} \right) e^{-2|k|h_1 \sqrt{1 - c^2/c_{T1}^2}} = 0 \end{aligned} \quad (12)$$

and the two relations for the required constants

$$a_1 = \frac{\mu_1 \alpha_1 - \mu_1^{(s)} k^2 + \rho_1^{(s)} \omega^2}{\mu_1 \alpha_1 + \mu_1^{(s)} k^2 - \rho_1^{(s)} \omega^2} e^{-\alpha_1 h_1} a_2, \quad b = \frac{\mu_1 \alpha_1}{\mu_2 \alpha_2} (a_1 e^{-\alpha_1 h_1} - a_2) \quad (13)$$

where

$$c_s = \sqrt{\frac{\mu_1^{(s)}}{\rho_1^{(s)}}}, \quad l_d = \frac{\rho_1^{(s)}}{\rho_1}. \quad (14)$$

Here c_s is a shear wave speed in an elastic membrane associated to the Gurtin-Murdoch elasticity, and l_d is the so-called dynamic characteristic length.

Introducing the notations

$$m_{12} = \frac{\mu_1}{\mu_2}, \quad k_d = |k|l_d, \quad h = nl_d, \quad (15)$$

and performing the scaling

$$v = \frac{c}{c_{T1}}, \quad v_s = \frac{c_s}{c_{T1}}, \quad v_r = \frac{c_{T2}}{c_{T1}}, \quad (16)$$

we get the dispersion equation written in the dimensionless form as follows

$$\begin{aligned} & \left(\sqrt{1 - \frac{v^2}{v_r^2}} + m_{12} \sqrt{1 - v^2} \right) \left(\frac{1}{k_d} \sqrt{1 - v^2} + v_s^2 - v^2 \right) \\ & + \left(\sqrt{1 - \frac{v^2}{v_r^2}} - m_{12} \sqrt{1 - v^2} \right) \left(\frac{1}{k_d} \sqrt{1 - v^2} - v_s^2 + v^2 \right) e^{-2nk_d \sqrt{1 - v^2}} = 0. \end{aligned} \quad (17)$$

Let us consider some particular cases. If $m_{12} \rightarrow \infty$ (i.e., $\mu_2 \rightarrow 0$), then (17) degenerates into the equation (compare with Eq. (3.15) in Mikhasev et al. (2022))

$$\frac{1}{k_d} \sqrt{1 - v^2} + v_s^2 - v^2 - \left(\frac{1}{k_d} \sqrt{1 - v^2} - v_s^2 + v^2 \right) e^{-2nk_d \sqrt{1 - v^2}} = 0 \quad (18)$$

45 for the layer with free bottom surface (see boundary condition (7)) without taking into account the surface effects.

On the other hand, when $m_{12} \rightarrow 0$, we arrive at the dispersion equation (see Eq. (3.7) in Mikhasev et al. (2022))

$$\frac{1}{k_d} \sqrt{1 - v^2} + v_s^2 - v^2 + \left(\frac{1}{k_d} \sqrt{1 - v^2} - v_s^2 + v^2 \right) e^{-2nk_d \sqrt{1 - v^2}} = 0 \quad (19)$$

for the layer with the bottom layer clamped in the x_3 -direction.

Passing to the limit as $n \rightarrow \infty$, we get the simple dispersion equation

$$\frac{1}{k_d} \sqrt{1 - v^2} + v_s^2 - v^2 = 0 \quad (20)$$

for the half-space with the shear modulus μ_1 and the density ρ_1 .

Finally, if $n \rightarrow 0$, then we obtain the following simple equation

$$\frac{1}{k_d} \sqrt{1 - \frac{v^2}{v_r^2}} + m_{12}(v_s^2 - v^2) = 0, \quad (21)$$

which is similar to Eq. (20). Reverting to the initial dimensional variables, it is easy to show that it coincides with the same dispersion equation as in Eremeyev & Sharma (2019), see Eq. (5),

$$\frac{c^2}{c_{T2}^2} = \frac{c_s^2}{c_{T2}^2} + \frac{\rho_2}{|k|\rho^s} \sqrt{1 - \frac{c^2}{c_{T2}^2}}, \quad (22)$$

but for the half-space with the shear modulus μ_2 and the density ρ_2 .



50 3. TH-TE regime of anti-plane waves

For the TH-TE regime, we seek solutions of Eqs. (4) in the form

$$u_1 = e^{i(kx_1 - \omega t)} (a_1 \sin \lambda x_2 + a_2 \cos \lambda x_2), \quad u_2 = b e^{i(kx_1 - \omega t)} e^{\alpha x_2}, \quad (23)$$

with a_1, a_2, b being constants.

Substituting (23) into Eqs. (4) gives

$$\lambda = |k| \sqrt{\frac{c^2}{c_{T1}^2} - 1}, \quad \alpha = |k| \sqrt{1 - \frac{c^2}{c_{T2}^2}}. \quad (24)$$

It can be seen that for the TH-TE regime $c_{T1} < c < c_{T2}$, i.e., the velocity of anti-plane shear wave is larger than the velocity of shear waves in the upper layer and less than the velocity of shear waves in the half-space.

Satisfying the boundary conditions (5)–(7) with (24) taken into account, we observe the following dispersion equation

$$\begin{aligned} & m_{12} \sqrt{\frac{c^2}{c_{T1}^2} - 1} \left(\sqrt{\frac{c^2}{c_{T1}^2} - 1} \tan \left(|k| h \sqrt{\frac{c^2}{c_{T1}^2} - 1} \right) - |k| l_d \left(\frac{c_s^2}{c_{T1}^2} - \frac{c^2}{c_{T1}^2} \right) \right) \\ &= \sqrt{1 - \frac{c^2}{c_{T2}^2}} \left(\sqrt{\frac{c^2}{c_{T1}^2} - 1} + |k| l_d \left(\frac{c_s^2}{c_{T1}^2} - \frac{c^2}{c_{T1}^2} \right) \tan \left(|k| h \sqrt{\frac{c^2}{c_{T1}^2} - 1} \right) \right) \end{aligned} \quad (25)$$

and the relations for the constants in (23) as

$$a_2 = b, \quad a_1 = \frac{\mu_2}{\mu_1} \frac{\alpha}{\lambda} b. \quad (26)$$

For the subsequent analysis, it is convenient to rewrite the dispersion Eq. (25) in the dimensionless form

$$\begin{aligned} & m_{12} \sqrt{v^2 - 1} \left(\sqrt{v^2 - 1} \tan \left(n k_d \sqrt{v^2 - 1} \right) - k_d (v_s^2 - v^2) \right) \\ & - \sqrt{1 - \frac{v^2}{v_r^2}} \left(\sqrt{v^2 - 1} + k_d (v_s^2 - v^2) \tan \left(n k_d \sqrt{v^2 - 1} \right) \right) = 0. \end{aligned} \quad (27)$$

55 We note that, in contrast to the TE-TE regime, Eq. (27) does not have any solution if the shear wave velocities of the upper layer and half-space

coincide ($v_r = 1$). The limiting case when the upper layer degenerates into the half-space ($n \rightarrow \infty$) should also be excluded.

Let us consider again some particular cases. Let $m_{12} \rightarrow 0$. Then Eq. (27) admits a very simple form,

$$\tan\left(nk_d\sqrt{v^2-1}\right) = \frac{\sqrt{v^2-1}}{k_d(v^2-v_s^2)}, \quad (28)$$

60 which coincides with equation (3.10) derived in Mikhasev et al. (2022) for the TH regime in the single layer with the bottom face clamped in the x_3 -direction.

If $m_{12} \rightarrow \infty$, then we get the novel equation

$$\tan\left(nk_d\sqrt{v^2-1}\right) = -\frac{k_d(v^2-v_s^2)}{\sqrt{v^2-1}}, \quad (29)$$

which goes for TH regime in the single elastic layer with free bottom face without taking into account surface effects.

65 Finally, letting the upper layer vanish, i.e. $n \rightarrow 0$, we again arrive at Eq. (22), which is not valid for the TH regime, but can be used for the TE regime of the anti-plane waves in the half-space with the shear modulus μ_2 and the density ρ_2 .

4. Dispersion curves analysis

4.1. TE-TE regime

70 Let us now consider the dispersion relation (17) corresponding to the TE-TE regime. First, we note that it has the root $v = 1$ (here $c = c_{T1}$) which should be excluded. Indeed, if $c = c_{T1}$, then $\alpha_1 = 0$ and, as follows from Eqs. (13), we get $u_1 = u_2 = 0$. Second, the numerical analysis of the dispersion Eq. (17) reveals that it does not have any positive roots if 75 $v_r < 1$, i.e., for $c_{T1} > c_{T2}$. So, all subsequent calculations are performed for parameters satisfying the nonstrict inequality $c_{T1} \leq c_{T2}$.

In Figure 2, the dimensionless velocity $v = c/c_{T1}$ versus the dimensionless wave parameter k_d is plotted at the fixed parameters $v_s = 0.25$, $m_{12} = 0.5$, $n = 20$ and for different values of the ratio $v_r = c_{T2}/c_{T1} = 1.005, 1.01, 1.05, 1.1$ (curves 1, 2, 3 and 4, respectively) of the shear waves velocities in the half-space and the upper layer. In Fig. 2 a), the dashed line corresponds 80 to the case when the velocities of shear waves in the layer and half-space are

the same, with mechanical properties being different. In the chosen scale, curve 4 merges with all dispersion curves for $v_r \geq 1.1$. Thus, the dashed line and the curve 4 can be considered as the lower and upper bounds, respectively, for the family of dispersion lines with different parameters v_r . Figure 2

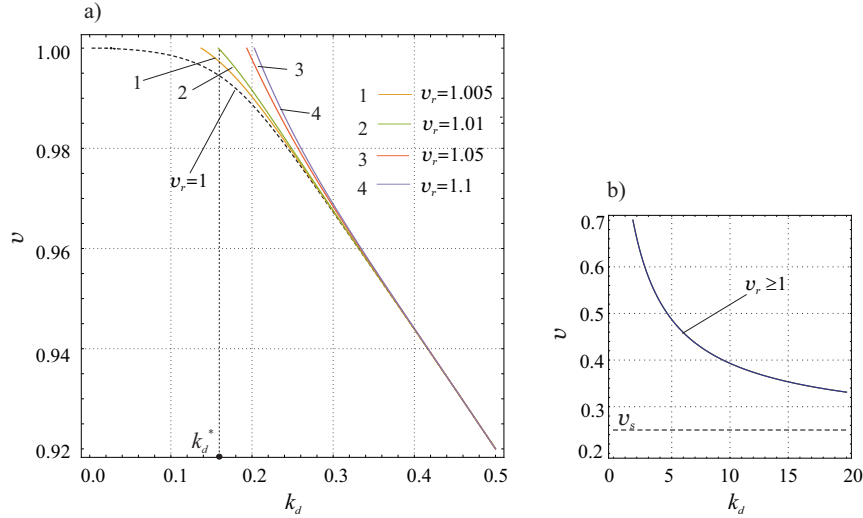


Figure 2: Dimensionless phase velocity $v = c/c_{T1}$ for TE-TE regime *vs.* wave number $k_d = |k|l_d$ for different ratios of the shear waves velocities in the half-space and the upper layer: a) Curves 1,2,3 and 4 correspond to ratios $v_r = 1.005, 1.01, 1.05$ and 1.1 , respectively; the dashed curve marked by $v_r = 1$ corresponds to the case when the shear wave velocities in the upper layer and the half-space are the same; b) Dispersion curves for large values of k_d .

b) shows that all dispersion curves asymptotically converge to the straight line $v = v_s$ (here, $v_s = 0.25$) as $k_d \rightarrow \infty$.

As expected, under fixed geometrical and physical parameters of the medium, the velocity c is a monotonically decreasing function of the wave parameter k_d . It is also seen that increasing the shear wave velocity c_{T2} in the half-space results in increasing the velocity c of the anti-plane shear waves.

Another interesting observation coincides with similar results by Mikhasev et al. (2022): for any fixed speed ratio v_r , there exists such a wave parameter k_d^* , that Eq. (17) does not have solutions at the segment $k_d \in [0, k_d^*]$. The behaviour of the dispersion curve near the point $(k_d^*, 1)$ can be approximated by the linear function

$$v = 1 - A\xi + O(\xi^2) \quad \text{as } \xi \rightarrow 0, \quad (30)$$

where $\xi = k_d - k_d^*$ with a parameter k_d^* to be determined and A is a constant.

Substituting (30) into Eq. (17) and equating coefficients in powers of $\xi^{1/2}$, we obtain the asymptotic relation for the point

$$k_d^* = \frac{\sqrt{m_{12}^2(1 - v_s^2)^2 v_r^2 + 4n(1 - v_s^2)(v_r^2 - 1)} - m_{12}v_r(1 - v_s^2)}{2n(1 - v_s^2)\sqrt{v_r^2 - 1}}. \quad (31)$$

The equation for the positive parameter A is not given here, since it is very cumbersome.

In Figure 3, the dispersion curves are drawn for $v_r = 2$, $v_s = 0.25$, $m_{12} = 0.5$ and different values of the parameter $n = h/l_d = h\rho_1/\rho_1^{(s)} = 0.025, 0.25, 0.5, 1$. The upper and lower dashed lines correspond to the cases when the elastic layer vanishes ($h \rightarrow 0$) or degenerates into a half-space ($h \rightarrow \infty$). These lines are plotted by solving Eqs. (21) and (20), respectively. It is seen

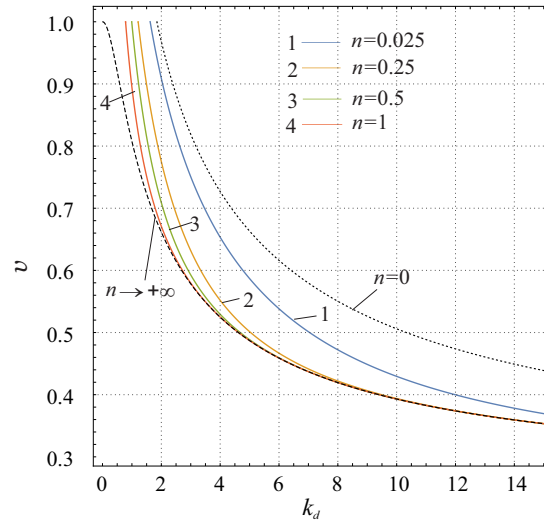


Figure 3: Dimensionless phase velocity $v = c/c_{T1}$ for TE-TE regime *vs.* wave number $k_d = |k|l_d$ for different values of the parameter $n = h/l_d = h\rho_1/\rho_1^{(s)} = 0.025, 0.25, 0.5, 1.1$.

that the velocity of anti-plane waves decreases when the thickness of the upper layer increases, and converges to the dashed line. Independent of the value of n , all curves converge to the straight line $v = v_s$.

Finally, Fig. 4 demonstrates the behaviour of the dispersion curves at different values of the ratio $m_{12} = \mu_1/\mu_2 = 0.5, 1, 2, 5$ and the fixed parameters $v_s = 0.25$, $n = 20$, $v_r = 2$. The upper and lower dashed lines plotted by solving Eqs. (19) and (18) are related to the limiting cases when $m_{12} \rightarrow 0$ and

$m_{12} \rightarrow \infty$, respectively. It is of interest to note that the lower dashed line

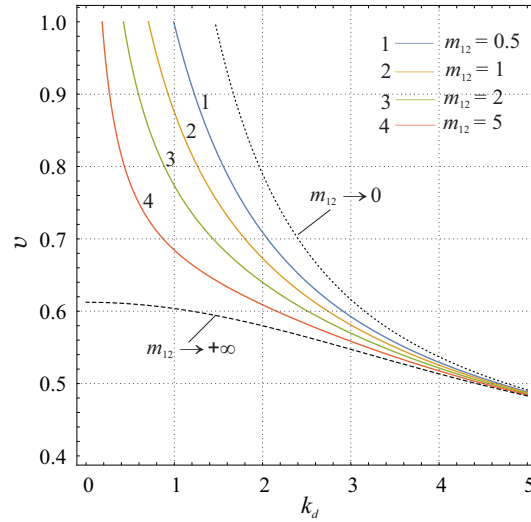


Figure 4: Dimensionless phase velocity $v = c/c_{T1}$ for TE-TE regime *vs.* wave number $k_d = |k|l_d$ for different values of the parameter $m_{12} = \mu_1/\mu_2 = 0.5, 1, 2, 5$.

gives the phase velocities in the elastic layer with free surfaces, of which the
 110 upper one has the surface enhancement (within the Gurtin-Murdoch model),
 while the lower one does not.

4.2. TH-TE regime

Let us analyze the dispersion curves for the TH-TE regime. Figure 5
 displays the solution of Eq. (27) with respect to v as the function of the
 115 wave parameter k_d for different values of the wave velocities ratio $v_r =$
 $1.05, 1.1, 1.5, 1.5$. The calculations were performed at $v_s = 0.5, m_{12} =$
 $0.5, n = 5$. The dashed curves correspond to the case when $v_r \rightarrow +\infty$. The
 curves lying above the straight line $v = 1$ are related to the TH-TE regime,
 while the curves below this line go for the TE-TE regime. It is of interest to
 120 note that the TE-TE curves plotted by solving Eq. (17) are continuations of
 the left family of the TH-TE curves.

In contrast to TE-TE regime, for each fixed value v_r there are the family
 (an infinite number) of the dispersion curves corresponding to TH-TE regime.
 Each dispersion line begins from some point (k_d^*, v_r) (which is removed). The
 point k_d^* is readily found by the asymptotic estimation of the dispersion curve

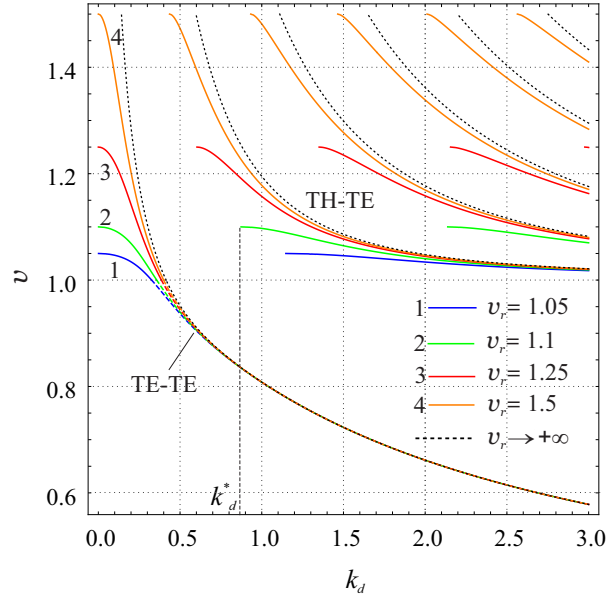


Figure 5: Dimensionless phase velocity $v = c/c_{T1}$ for TH-TE and TE-TE regimes *vs.* wave number $k_d = |k|l_d$ for different ratios of the shear waves velocities in the half-space and the upper layer. Curves 1,2,3, and 4 correspond to ratios $v_r = 1.005, 1.1, 1.25$ and 1.5 , respectively. The dashed curves correspond to the limit case when $v_r \rightarrow \infty$.

behaviour in the neighbourhood of the point (k_d^*, v_r) . Let

$$v = v_r - A\xi + O(\xi^2), \quad \xi = k - k_d^*. \quad (32)$$

We substitute (32) into Eq. (27) and expand all parameters depending on ξ into the series in powers of $\xi^{1/2}$. Considering only the leading approximation, we straightaway arrive at the equation with respect to the required k_d^* :

$$\tan\left(nk_d^*\sqrt{v_r^2 - 1}\right) = \frac{k_d^*(v_s^2 - v_r^2)}{\sqrt{v_r^2 - 1}}. \quad (33)$$

The constant A can be determined from the next two approximations, however because of cumbersome calculations we omit it here.

125 Figure 6 shows the behaviour of the dispersion curves, mainly for the TH-TE regimes, for different values of the parameter $n = 20, 10, 5$ (blue, green and red lines marked by 1, 2 and 3, respectively) specifying the thickness of the upper layer. Here the input parameters are the following: $v_s = 0.25, m_{12} = 0.5, v_r = 2$. The dashed black line, plotted by solving Eq. (22), is

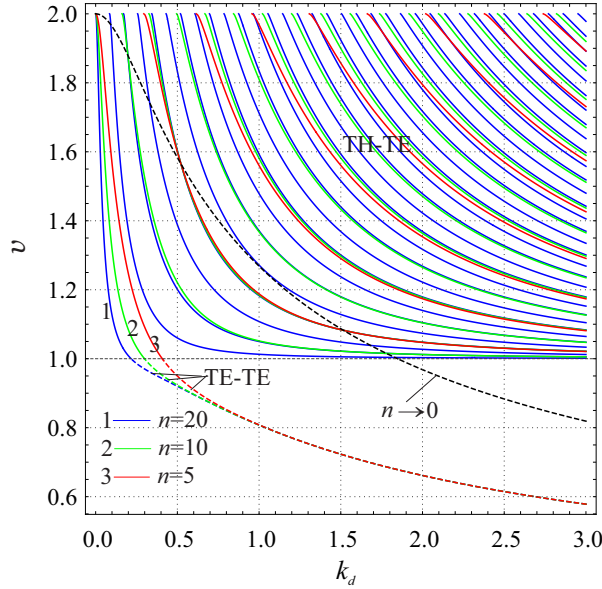


Figure 6: Dimensionless phase velocity $v = c/c_{T1}$ for TH-TE and TE-TE regimes vs. wave number $k_d = |k|l_d$ for different values of the parameter $n = 20, 10, 5$ (curves 1, 2, 3, respectively). The dashed black curve corresponds to the limit case when $n \rightarrow 0$.

related to the case when the upper layer vanishes ($h \rightarrow 0$). We note that the
 130 left family of the TH-TE curves (which continuously transfer into the TE-
 TE lines below the straight line $v = 1$) starts from the point $(0, v_r)$ (here,
 $v_r = 2$) regardless of the thickness parameter n . The smaller the thickness
 h , the rarer the corresponding family of dispersion curves beginning from
 the point (k_d^*, v_r) with $k_d^* > 0$ becomes. In the limit, as $h \rightarrow 0$, all disper-
 135 sion curves to right of the dashed line and corresponding to only the TH-TE
 regime degenerate into this dashed line, which, however, is not a dispersion
 curve.

The effect of varying the elastic moduli ratio $m_{12} = \mu_1/\mu_2$ on the dimen-
 sionless phase velocity v is shown in Figure 7. The input parameters are
 140 $v_s = 0.25, n = 2$ and $v_r = 2$. The curves marked by 1, 2, 3 and 4 correspond
 to the ratios m_{12} equal to 0.03, 0.1, 1 and 2, respectively. The dashed black
 curves are related to the limit case as $m_{12} \rightarrow \infty$, and the black dash-dotted
 lines go for the case when $m_{12} \rightarrow 0$. The corresponding dispersion relations
 for these cases are Eqs. (29) and (28), respectively. The curves above and
 145 below the straight line $v = 1$ correspond to the TH-TE and TE-TE regimes,
 respectively. It may be seen that for the fixed values of the parameters

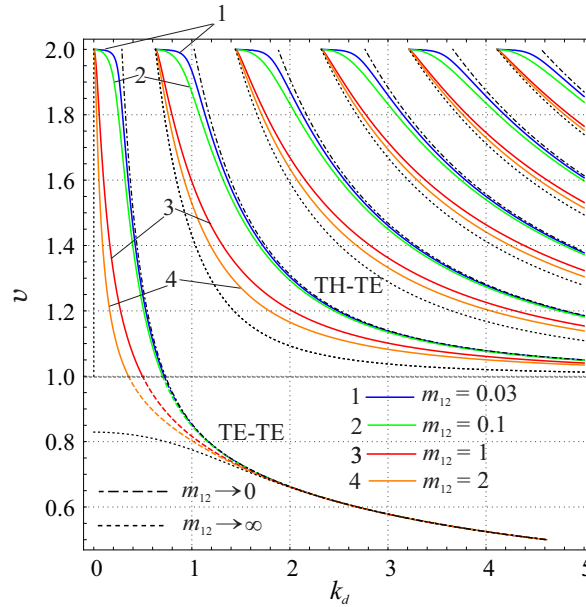


Figure 7: Dimensionless phase velocity $v = c/c_{T1}$ for TH-TE and TE-TE regimes *vs.* wave number $k_d = |k|l_d$ for different values of the parameter $m_{12} = 0.03, 0.1, 1, 2$ (blue, green, red and brown curves marked by 1, 2, 3, and 4, respectively). The dashed black curves correspond to the limit case when $m_{12} \rightarrow \infty$, and the black dash-dotted lines are related to the case $m_{12} \rightarrow 0$.

v_s, n, v_r , the dispersion curves related to TH-TE regime for any ratio m_{12} get into one of the series of narrow domains which are bounded by the dashed and dash-dotted lines. The numerical experiments show that the thicker the elastic layer attached to the half-space (under other fixed input parameters), the more narrow each of these domains become. As $k_d \rightarrow \infty$, all curves related only to TH-TE regime together with the dashed and dash-dotted lines converge to the straight line $v = 1$, while the curves getting from the TH-TE regime into TE-TE one converge to the line v_s . Thus, with increasing wavenumber, the influence of the moduli ratio $m_{12} = \mu_1/\mu_2$ on the phase velocity c of the anti-plane waves weakens.

Conclusions

We discussed the propagation of anti-plane surface waves, i.e. waves localized in the vicinity of a free surface, in a layered elastic medium which consists of a layer of finite thickness perfectly attached to a half-space. In

addition we also assume action of surface stresses on the free surface of the layer. The Gurtin–Murdoch model is utilized here. The latter play a crucial role here, since they corresponds to the new type of shear surface waves. We derived dispersion relations and presented the complete picture of dispersion curves. The presence of surface stresses brings additional characteristic length-scale parameters in the model. As a result, we have two regimes called transversally exponential (TE) and transversally harmonic (TH) described by exponential and trigonometric functions, respectively. TE regime corresponds to surface waves propagated with lower speed than ones in TH regime. Since TE regime is determined by surface properties, these could be useful experimental determination of surface moduli and of surface material properties of multilayered coating, in general.

Acknowledgments

G.M. acknowledges the support from the Scientific and Research Council of Turkey in the framework of Visiting Scientist Programme BIDEB 2221 V.A.E. acknowledges the support of the Royal Society Wolfson Visiting Fellowships program under the Project CR\212159 “Modelling of complex multiphysical phenomena on microstructured surfaces”.

References

- Achenbach, J. (1973). *Wave Propagation in Elastic Solids*. Amsterdam: North Holland.
- Eremeyev, V. A., Rosi, G., & Naili, S. (2016). Surface/interfacial anti-plane waves in solids with surface energy. *Mechanics Research Communications*, *74*, 8–13.
- Eremeyev, V. A., & Sharma, B. L. (2019). Anti-plane surface waves in media with surface structure: Discrete vs. continuum model. *International Journal of Engineering Science*, *143*, 33–38.
- Gurtin, M. E., & Murdoch, A. I. (1975). A continuum theory of elastic material surfaces. *Arch. Ration. Mech. An.*, *57*, 291–323.
- Mikhasev, G. I., Botogova, M. G., & Eremeyev, V. A. (2022). Anti-plane waves in an elastic thin strip with surface energy. *Phil. Trans. R. Soc. A*, *380*, 20210373–15.

